J. Mater. Eng. (1987) 9:81–92

Effect of Composition on Thermal Expansion of Alloys Used in Power Generation

F.C. Hull, S.K. Hwang, J.M. Wells, and R.I. Jaffee

Abstract. A study based on published data was conducted of the effects of chemical composition on thermal expansion of several groups of alloys: austenitic stainless steels, nickel-base nonmagnetic alloys, ferritic and martensitic irons and steels, duplex stainless steels, and FCC magnetic alloys. Computer regression analyses were performed on the first three of these groups to establish models to predict the mean thermal expansion coefficient ($\bar{\alpha}$) from the composition. The models predict $\bar{\alpha}$ with a standard error of 0.19–0.23 $\times$ 10^{-6}/°F, which is comparable to the standard error of experimental measurements of $\bar{\alpha}$. The most influential elements for each group are Ni (for decreasing $\bar{\alpha}$) in the austenitic steels group, Mo (decreasing) in the nickel-base nonmagnetic alloys group, and Cr (second-order decreasing effect) in the ferritic and martensitic irons and steels group. The models should be useful in system designs involving combined use of austenitic and ferritic alloys in high-temperature structures, such as for maintaining clearances or interference fits or for minimizing cyclic stresses. The equations could also help a metallurgist develop an alloy with a specified thermal expansion coefficient.

INTRODUCTION

It is common knowledge that ferritic materials have lower coefficients of thermal expansion than austenitic stainless steels and that nickel-base alloys have coefficients somewhere in between. Figure 1 illustrates this point, as well as the ranges of values encountered within groups of alloys. However, within a given class of materials, it was believed there was little systematic variation of $\bar{\alpha}$.

In 1979, at the Westinghouse R&D Center, an exploratory modeling study was conducted to discover if the $\bar{\alpha}$ of the austenitic member could be controlled through composition to provide a solution to the generic problem of the differences in $\bar{\alpha}$ between ferritic and austenitic steels. The study consisted of (1) a compilation of data on $\bar{\alpha}$ of nonmagnetic, nickel-base alloys and stainless steels with a FCC structure, (2) regression modeling of the effects of alloying elements on $\bar{\alpha}$, and (3) experimental verification and refinement of the regression models on nonmagnetic, nickel-base experimental alloys. From these studies it was found that the prediction of $\bar{\alpha}$ in these alloys was feasible [1–3].

The Electric Power Research Institute (EPRI) funded a program in 1983 to broaden the base of the previous study to include other types of alloys used in power generation equipment, including ferritic and martensitic irons and steels, ferritic and martensitic stainless steels, superalloys, austenitic and duplex austenitic-ferritic steels, to determine if equations could be developed to calculate $\bar{\alpha}$ from the composition of these steels. The usefulness of such information is clear. Much utility equipment must be made of different materials. Dissimilar metal welds are utilized in boiler superheaters and reheaters and in turbine sleeves connecting austenitic to ferritic steels. Frequently, in high-temperature turbines, it is necessary to use ferritic casings to enclose austenitic rotors, which may well be the case in advanced steam plants. High-temperature bolts made of austenitic steel used with ferritic casings are another example. In thermal stress calculations, there is frequently a need for expansion coefficients of special alloys not readily available.

This paper is a condensation of the salient points of the final report to EPRI. For additional details and

F.C. Hull, J.M. Wells, and S.K. Hwang were formerly with the Westinghouse R&D Center, Pittsburgh, PA. F.C. Hull is now a consultant; S.K. Hwang is with the Dept. of Metallurgy, Inha University, Inchon, Korea; and J.M. Wells is with the U.S. Army Materials Technology Lab, Watertown, MA. R.I. Jaffee is with the Electric Power Research Institute, Palo Alto, CA.

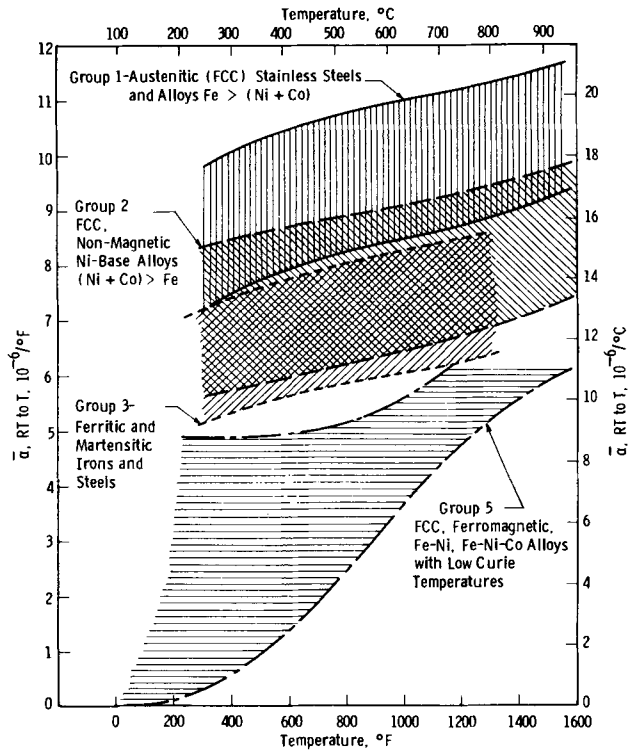

Fig. 1. Ranges of mean thermal expansion coefficient ($\bar{\alpha}$) from room temperature to T of austenitic stainless steels, FCC nonmagnetic Ni-base alloys, ferritic and martensitic irons and steels, and FCC ferromagnetic Fe-Ni and Fe-Ni-Co alloys.

for complete tabulation of thermal expansion and composition data on 1036 materials, reference should be made to the EPRI report [4].

TECHNICAL APPROACH

Classification of Alloys

Alloys were divided into the following groups based primarily on their chemical composition (Fe-base vs. Ni-base), crystal structure (FCC vs. BCC), and whether they were paramagnetic or ferromagnetic. For all except group 4 alloys, the indicated figure shows the temperature dependence of $\bar{\alpha}$ (RT to T) for representative alloys of each group. For group 1, 2, and 3 alloys, the curves within a group tend to have the same slope and are only displaced to higher or lower $\bar{\alpha}$ as a result of composition changes. In contrast to this behavior, the curves of the alloys of group 5 have widely different slopes and shapes.

Group 1: Austenitic (FCC), iron-base, nonmagnetic alloys with Fe > (Ni + Co) (Fig. 2).

Group 2: FCC, nickel-base, nonmagnetic alloys with (Ni + Co) > Fe (Fig. 3).

Group 3: Ferritic and martensitic stainless irons and steels and high-alloy and low-alloy irons and steels (Fig. 4).

Group 4: Duplex stainless steels with austenite and a high percentage of delta ferrite.

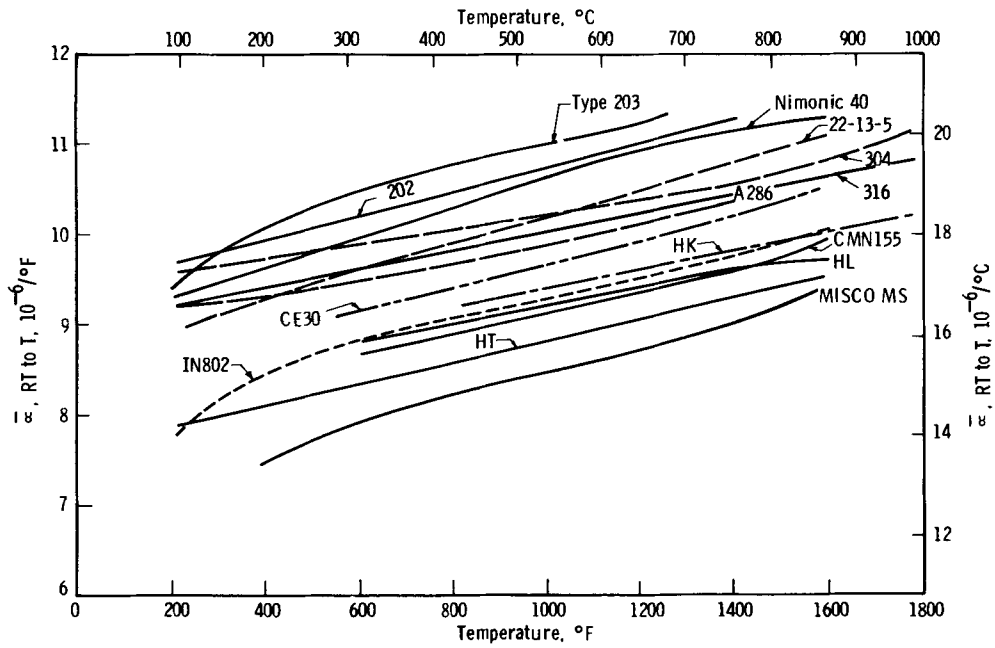

Fig. 2. Mean thermal expansion coefficients of representative nonmagnetic, austenitic steels (group 1).

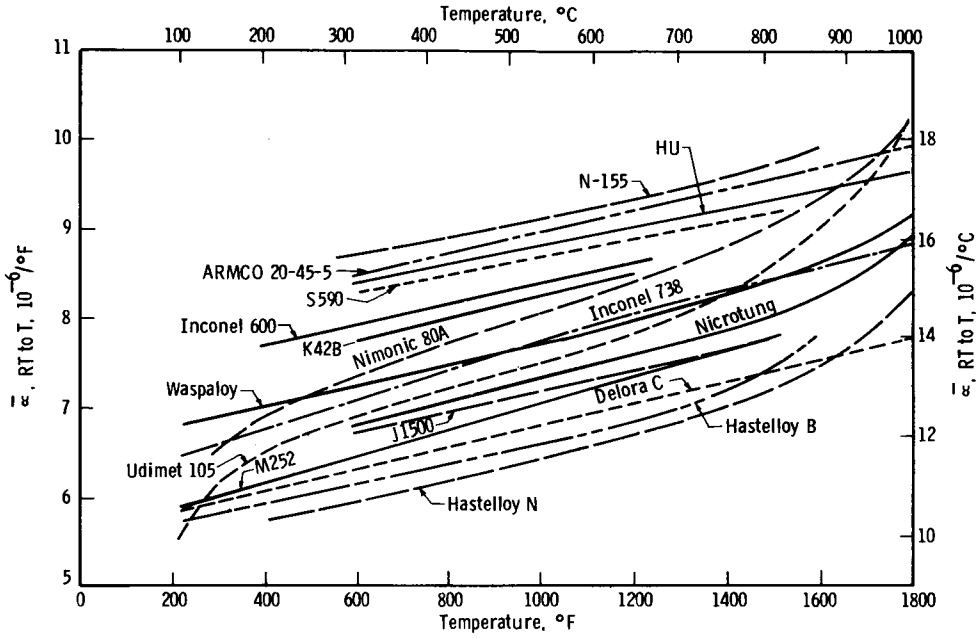

Fig. 3. Mean thermal expansion coefficients of representative nonmagnetic, FCC Ni-base alloys (group 2).

Group 5: FCC, Fe-Ni, and Fe-Ni-Co ferromagnetic alloys with a low Curie temperature (Fig. 5).

Compilation of Data

Thermal expansion and composition data were obtained from a variety of handbooks [5–8], published articles, U.S. patents, and manufacturer's data sheets [9,10]. The composition terms selected for the data file and regression analysis were Ni, Co, Cr, Mo, W, Fe, Ti, Al, Nb, Ta, Mn, Si, C, Cu, V, and N. These include Fe, Ni, and Co and combinations of these for base compositions; Cr, Mo, W, and V for solid solution hardening, hardenability, or carbide formation; Ti, Al, Nb, Ta, and Cu for precipitation hardening;

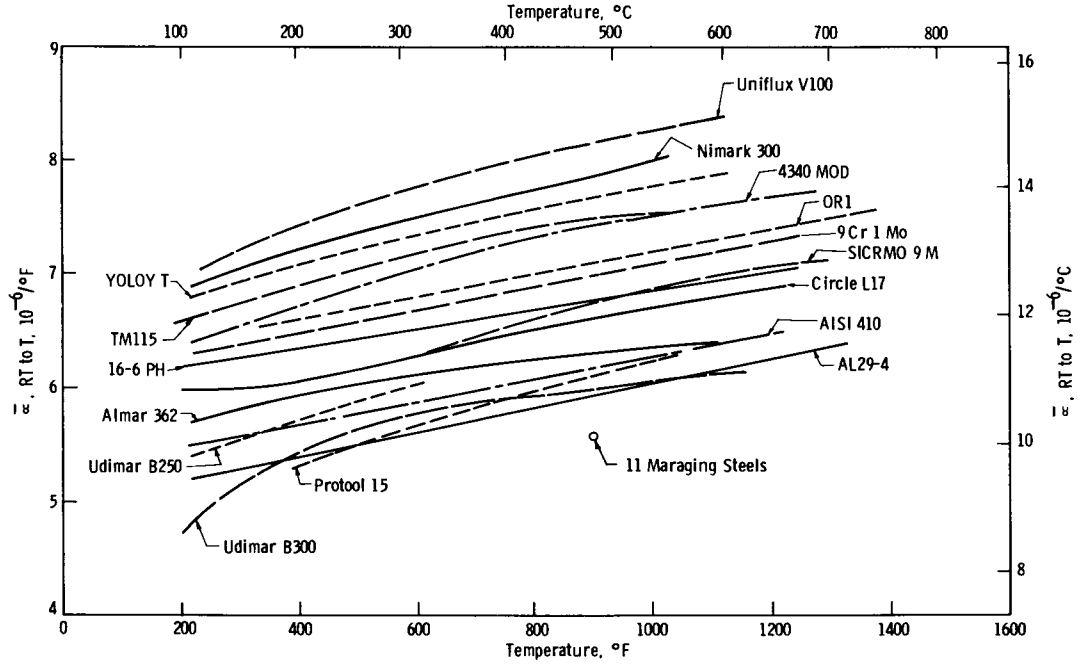

Fig. 4. Mean thermal expansion coefficients of representative ferritic and martensitic low-alloy irons and steels (group 3).

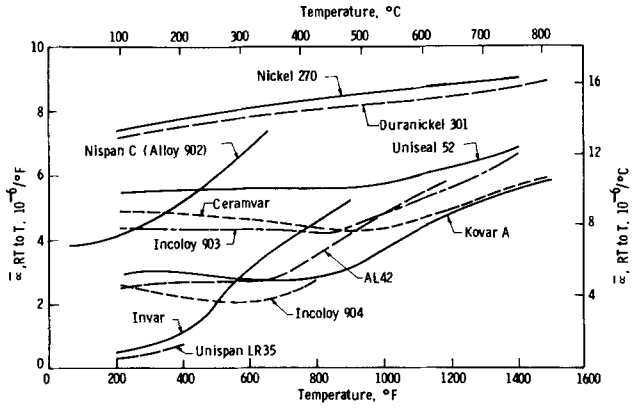

Fig. 5. Mean thermal expansion coefficient of FCC magnetic alloys (group 5).

Mn and Si as deoxidizers; and Mn and N as austenitizers in low-Ni stainless steels. Impurities, such as P and S, and trace elements, such as B, Ca, Mg, Pb, Se, and Zr, are usually present in too small an amount to influence $\bar{\alpha}$.

Our main objective was to obtain values of $\bar{\alpha}$ from room temperature (*RT*) to 1000° F (538° C), since this is the temperature range of interest for current steam power plants. As data were available, the range was extended to 1200° F (649° C), which would encompass peak temperatures for advanced steam cycle plants and down to 600° F (316° C) and 800° F (427° C) to include nuclear applications and lower-temperature portions of conventional plants.

Regression Modeling

In order to quantitatively evaluate the effects of composition on $\bar{\alpha}$, within a given alloy group, it was assumed that $\bar{\alpha}$ was linearly related to a number of composition terms, which included a constant, linear, and squared terms and interactions, e.g.,

$$\bar{\alpha} = \beta_0 + \beta_1 A + \beta_2 A^2 + \beta_3 B + \beta_4 B^2 + \beta_5 AB + \beta_6 C + \ldots$$

where β_0, β_1, β_2 ... are the regression coefficients and *A*, *B*, *C* ... represent the alloying elements. BMDP statistical computer programs [11] were used to determine the regression coefficients. Within the BMDP regression programs, the subprograms of multiple linear regression (*P1R*) and all possible subsets regression (*P9R*) were utilized extensively in the present work. The criterion for selecting terms in the regression models was that the correlation coefficient, *R*, of the model as a whole be a maximum and the *T* significance of the coefficient of each term in the model be greater than 1.5. Selection of a specific model required iterative computer runs using *P1R* and *P9R* programs.

MODELING OF THE EFFECT OF COMPOSITION ON THERMAL EXPANSION

For the alloy types for which modeling was attempted, groups 1, 2, and 3, the ranges of the input variables are shown in Table I. Since the ranges of the concentration did not vary significantly between the data bases for the $\bar{\alpha}$'s of different temperatures, only the summaries of the data used for modeling TEC 1000 (mean thermal expansion from *RT* to 1000° F) are presented. In the computer modeling, the base metal elements (Fe for groups 1 and 3 and Ni for group 2) were deliberately deleted from the list of the independent variables.

Group 1: Fe-Base Nonmagnetic Steels

Table II presents the models for calculating $\bar{\alpha}$ from the alloy composition and shows the standard error (SE) of predicting $\bar{\alpha}$ for each temperature and for each alloy group. However, within each model, the significance and SE of the terms vary considerably, as shown in Table III for TEC 1000 of group 1 alloys.

Although the Ni term in the equation for TEC 1000 of group 1 alloys has the highest significance and the smallest SE, there is still considerable scatter in the plot of observed and predicted $\bar{\alpha}$ as a function of Ni content, as shown in Figure 6. However, the role of Ni in decreasing $\bar{\alpha}$ is unmistakable. For similar details

Table I. Ranges of Composition of Input Data for Modeling Studies of TEC 1000 of Group 1, 2, and 3 Alloys in Weight Percent

	Group 1		Group 2		Group 3	
Element	Min.	Max.	Min.	Max.	Min.	Max.
Ni	1.4	38.0	0	95.0	0	18.5
Co	0	0	0	65.6	0	9.0
Cr	8.0	30.0	0	36.5	0	29.0
Mo	0	4.5	0	32.0	0	5.0
W	0	0	0	15.0	0	4.0
Fe	33.3	74.4	0	38.6	62.9	99.8
Ti	0	4.0	0	5.0	0	1.2
Al	0	1.2	0	6.5	0	3.9
Nb	0	1.0	0	5.3	0	1.0
Ta	0	0.4	0	4.0	0	1.0
Mn	0	14.8	0	11.0	0	2.0
Si	0	2.3	0	4.0	0	2.0
C	0	0.53	0	0.64	0	1.2
Cu	0	3.5	0	0.4	0	4.1
V	0	2.5	0	1.0	0	1.2
N	0	0.4	0	0	0	0.25
TEC 1000	8.50	11.05	5.90	9.20	5.62	8.42
No. of data	178		262		305	

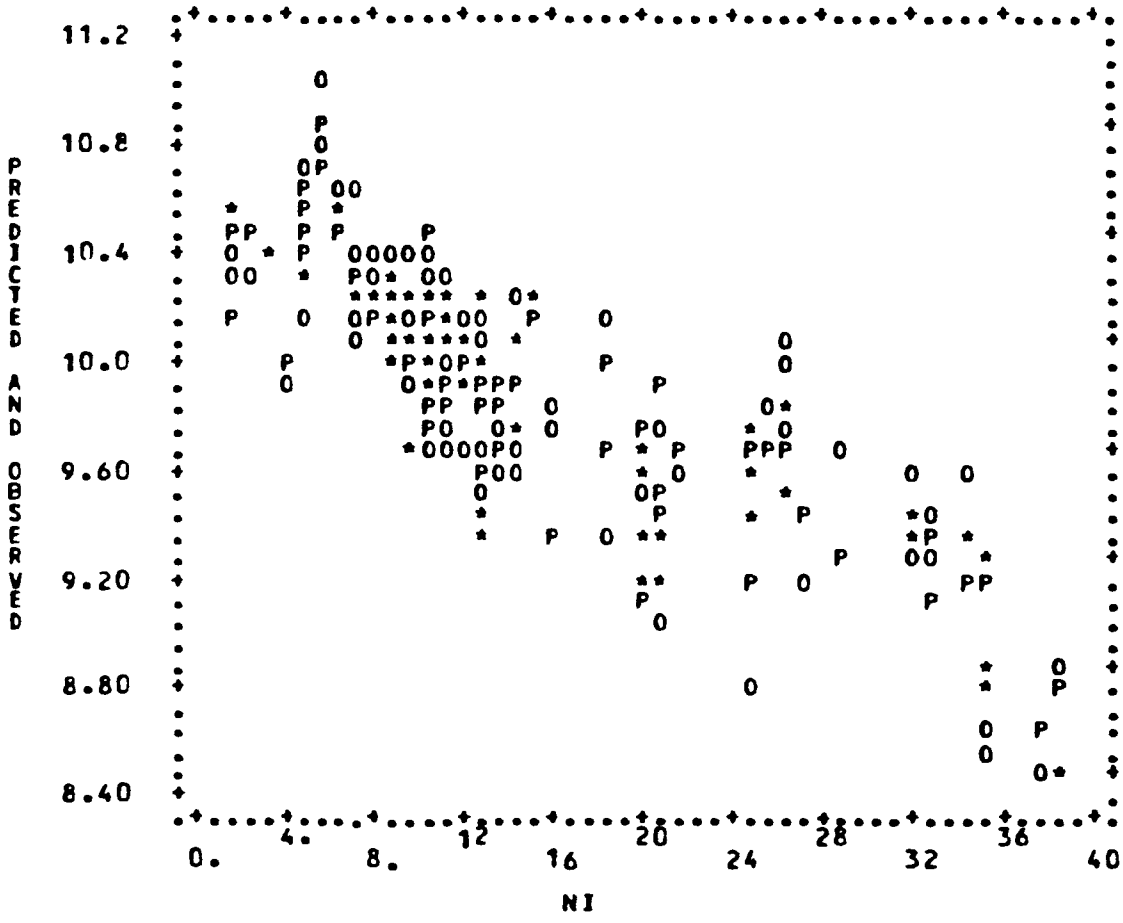

Fig. 6. Predicted (P) and observed (O) values of TEC 1000 for group 1 alloys as a function of Ni content (wt%). Asterisk indicates that the predicted and observed values coincided.

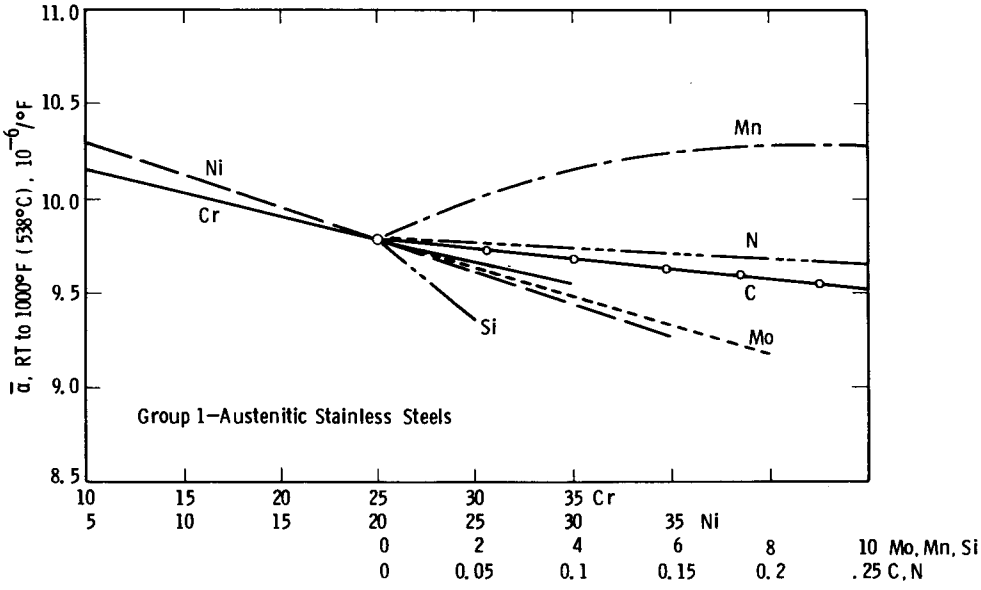

Fig. 7. Effect of composition on ᾱ of a group 1 austenitic stainless steel with 25Cr-20Ni balance Fe.

Table II. Results of Multiregression Analyses on TEC 600, 800, 1000, and 1200 of Group 1, 2, and 3 Steels (unit of coeff: 10^{-6}/°F)

	TEC 600			TEC 800			TEC 1000			TEC 1200		
Term	G1	G2	G3	G1	G2	G3	G1	G2	G3	G1	G2	G3
Intercept	11.936	8.013	7.314	11.855	8.072	7.592	11.080	8.133	7.904	11.344	8.419	8.047
Ni	−0.0380	NA	−0.0303	−0.0371	NA	−0.0391	−0.0338	NA	−0.0470	−0.0343	NA	−0.0503
Co	—	0.00496	−0.140	—	0.00338	−0.148	—	—	−0.134	—	—	−0.0972
Cr	−0.126	—	−0.125	−0.107	0.0158	−0.133	−0.0244	0.0253	−0.138	−0.0258	0.0302	−0.147
Mo	−0.107	−0.0735	—	0.0969	−0.0710	0.0263	−0.0762	−0.0656	—			
W	—	−0.0633	—	—	−0.0549	—	—	−0.0417	—	—	−0.0433	0.0342
Fe	NA	—	NA	NA	—	NA	NA	—	NA	NA	—	NA
Ti	—	−0.0935	0.208	—	−0.0971	0.261	—	−0.0925	0.308	—	−0.0948	0.381
Al	—	−0.0647	0.136	—	−0.0512	0.126	—	−0.0399	0.103	—	−0.0467	0.105
Nb + Ta	—	—	—	—	—	—	—	−0.0162	—	—	−0.0220	—
Mn	0.0634	—	—	0.0863	—	—	0.118	0.0607	—	0.0990	—	—
Si	−0.313	—	—	−0.287	—	—	−0.219	−0.0683	−0.111	−0.1223	—	—
C	−1.316	—	−0.160	−1.244	—	—	−1.042	—	—	−1.077	—	0.191
Cu	—	—	0.115	—	—	0.123	—	—	0.128	—	—	0.130
V	—	—	0.247	—	—	—	—	—	—	—	—	—
N	—	—	—	—	—	—	−0.543	—	—	—	—	—
Cr^2	0.00241	−0.000180	0.00306	0.00198	−0.000484	0.00308	—	−0.000535	0.00317	—	−0.000704	0.00345
Fe^2	NA	0.00329	NA	NA	0.000290	NA	NA	0.000376	NA	NA	0.00283	NA
Mn^2	−0.00570	—	—	0.00738	—	—	−0.00735	—	—	−0.00673	—	—
MoFe	NA	0.00324	NA	NA	0.00312	NA	NA	0.00245	NA	NA	0.00255	NA
SE	0.23	0.28	0.26	0.21	0.25	0.24	0.19	0.22	0.23	0.19	0.24	0.28
R^2	0.80	0.77	0.81	0.83	0.81	0.85	0.84	0.83	0.88	0.85	0.81	0.84
F-Ratio	78	72	138	84	80	207	114	114	267	113	80	164
No. of data	162	181	310	143	181	293	178	262	305	150	183	281

on other models and other elements, the reader should refer to Hwang et al [4].

The effects of composition on $\bar{\alpha}$ are shown graphically for group 1 alloys in Figure 7. For this example, a steel with 25Cr, 20Ni and balance Fe was chosen. Mn, N, C, Mo, or Si was added to the 25Cr-20Ni base in place of part of the Fe. Cr variations are shown for an alloy with 20Ni and balance Fe. Ni variations are likewise shown for an alloy with 25Cr and balance Fe.

Table III. Results of the Multiregression Analysis on TEC 1000 of Fe-Base Nonmagnetic Steels (group 1) (unit of Coeff: 10^{-6}/°F/wt%)

Terms	Coeff	SE	T
Intercept	11.080		
Ni	−0.0338	0.00191	−17.7
Cr	−0.0244	0.00488	−5.00
Mo	−0.0762	0.0134	−5.70
Mn	0.118	0.0224	5.25
Si	−0.219	0.0421	−5.21
C	−1.042	0.158	−6.58
N	−0.543	0.284	−1.91
Mn^2	−0.00735	0.00153	−4.79
SE of regression: 0.19			
F ratio: 114			
Multiple R^2: 0.84			
No. of data: 178			

In the absence of interactions between terms, the effects of several elements would be additive. Manganese had a significant second-order effect, with a maximum TEC 1000 at 8.0 pct Mn.

Group 2: Ni-Base, FCC, Nonmagnetic Alloys

The mean concentrations of Co and W in the input data for modeling TEC 1000 of the group 2 alloys were 9.2 and 1.5 pct, respectively. The mean concentration of Mo was about seven times that in the group 1 alloys. Other elements of significantly higher concentration in the group 2 alloys were the γ' or γ'' precipitation-hardening elements, Ti, Al, Nb, and Ta. On the other hand, the contents of C, Mn, and Si were comparatively lower in the group 2 alloys. The mean TEC 1000 for the group 2 alloys, 7.97×10^{-6}/°F, was about 20 pct lower than the mean TEC 1000 for the group 1 alloys.

The effects of composition on $\bar{\alpha}$ of group 2 alloys are illustrated in Figure 8. An alloy of 20Cr-80Ni was chosen as a base for this example. In these Ni-base, FCC, nonmagnetic alloys, Mo was found to have a significant effect. Other elements that tended to decrease $\bar{\alpha}$ were W, Ti, Al, (Nb + Ta), and Si. The alloying elements that tended to increase $\bar{\alpha}$ were Fe and Mn. Chromium showed a second-order effect peaking at 23.6 pct.

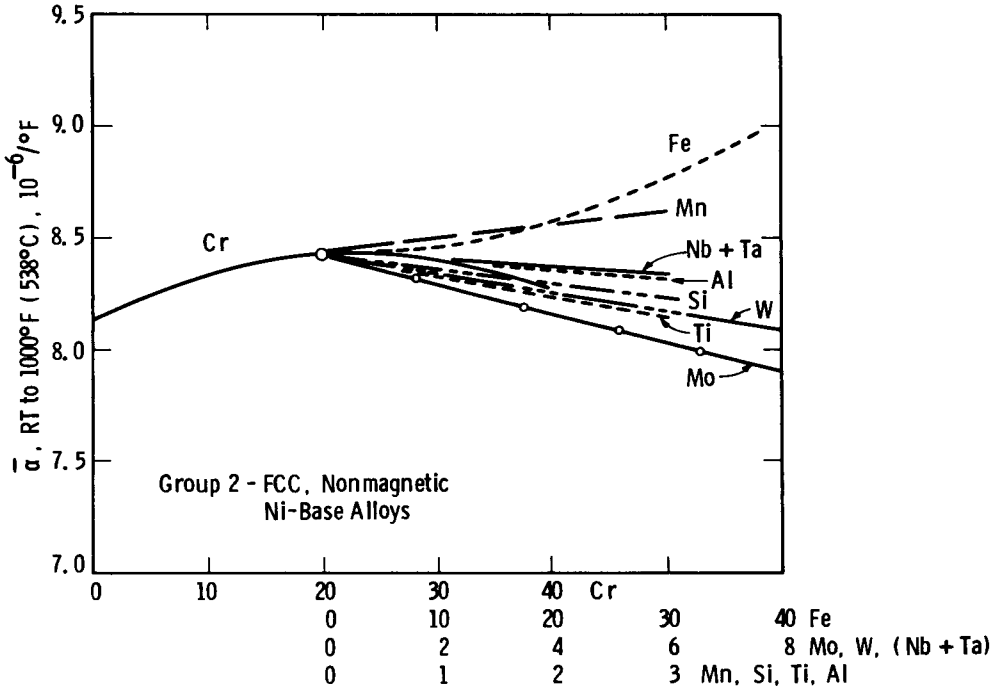

Fig. 8. Effect of composition on ᾱ of a FCC, nonmagnetic Ni-base alloy with 20Cr, balance Ni.

Morrow et al. [12] measured the effects of Mo, Al, and Ti on ᾱ of nickel-base alloys. In alloys containing 0 to 34 pct Co, 12 to 35 pct Cr, 0 to 9 pct Mo, 0 to 6 pct Al, and 0 to 4 pct Ti, they found that Mo decreased ᾱ of solid solution as well as γ′ precipitation-hardened alloys.

Group 3: Ferritic and Martensitic Stainless Irons and Steels and High-Alloy and Low-Alloy Irons and Steels

The mean contents of Ni and Cr in this alloy group were lower than those in the group 1 or group 2 alloys. The mean content of Co was lower than that of the group 2 alloys but was slightly higher than that of the group 1 alloys. In comparison to the former two groups, the mean concentration of C was the highest in the group 3 alloys because of the many carbon-strengthened steels. Also, the contents of Cu and V were higher than those in the former two groups of alloys, owing to the contribution from a number of precipitation-hardened ferritic or martensitic steels. The mean concentrations of Ti and Al were significantly lower than those of the group 2 alloys; however, they were comparable to those of the group 1 alloys. The mean thermal expansion coefficients of the group 3 alloys were lower than those of the group 1 or group 2 alloys.

The alloying elements that decreased ᾱ monotonically were Ni, Co, and Si. The elements that increased ᾱ monotonically were Ti, Al, and Cu. Chromium had a second-order effect, as shown in Figure 9, with a minimum at 21.8 pct. Since most alloys in group 3 are lean alloys of Fe, the effects of the alloying elements within their normal composition ranges are not pronounced, except for that of Cr.

Group 4: Duplex Stainless Steels

The compositions of austenitic stainless-steel weld metals are typically balanced to provide 2 to 10 pct delta ferrite in the weld deposit to minimize microfissuring. Similarly, austenitic stainless-steel castings

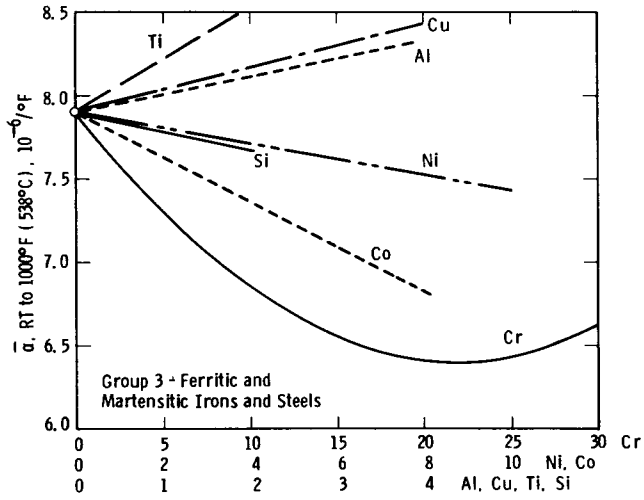

Fig. 9. Effect of composition on ᾱ of group 3 ferritic and martensitic irons and steels with balance Fe.

usually contain 8 to 15 pct delta ferrite to reduce hot tearing and to increase yield strength. Such alloys have been included with the group 1 alloys.

Although such welds and castings are often referred to as having duplex microstructures, the term "duplex" is more properly reserved for stainless steels containing substantial quantities of delta ferrite—up to 50 pct in some cases. Some typical duplex steels are listed in Table IV.

The literature provides few examples of group 4 duplex stainless steel for which thermal expansion data are available and the percent delta ferrite is specified. For these reasons, it was not possible to use the approach used for group 1, 2, and 3 alloys to correlate composition and $\bar{\alpha}$.

However, $\bar{\alpha}$ can be calculated using the rule of mixtures if the compositions of the two phases are known, as well as their relative proportions. Hayden and Floreen [13–15] have studied some microduplex stainless steels and developed tie-line positions in the (δ + γ) field. Figure 10 shows an isothermal section through the Fe-Ni-Cr phase diagram at 1700° F (927° C). An alloy of average composition *X* would contain 53 pct γ of composition *A* and 47% delta ferrite of composition *F*. Table V lists these three alloy compositions in weight percent.

The $\bar{\alpha}$ for the γ phase from *RT* to 1000° F (538° C) can be calculated by the model for group 1 alloys, and the $\bar{\alpha}$ for the delta ferrite can be calculated by the model for group 3 alloys. These results and values for intermediate compositions along the same tie line are given in Table VI.

The $\bar{\alpha}$ calculated for the average composition *X*, assuming the alloy was completely austenitic and nonferromagnetic, is 10.10×10^{-6}/°F as compared to 10.13×10^{-6}/°F for the average composition *A*. Thus it can be seen that composition per se has a minor effect on $\bar{\alpha}$, and the major difference is caused by the difference in $\bar{\alpha}$ between the austenitic, nonmagnetic versus the ferritic, ferromagnetic phase.

For other solution temperatures, for other Fe-Ni-Cr compositions, or for duplex alloys containing Mo, for example, additional phase diagram and tie-line information would be needed. Sources of such information are papers and books by Kaufman et al. [16,17] and the Manlabs interactive on-line, computer data bank for phase diagrams [18]. In the absence of the tie-line data, $\bar{\alpha}$ of duplex steels can be estimated by calculating an $\bar{\alpha}$ from the total alloy composition assuming 100 pct austenite (i.e., using the equations for group 1 alloys) and then subtracting 0.037×10^{-6}/°F for each percent delta ferrite in the actual microstructure.

At lower temperatures, such as would be encountered in conventional steam plants, the delta ferrite composition falls within *a* (δ + γ + σ) field of the phase diagram. Hull [19] has reported that such delta ferrite transforms rather readily to austenite plus sigma with a shrinkage of dimensions of the component.

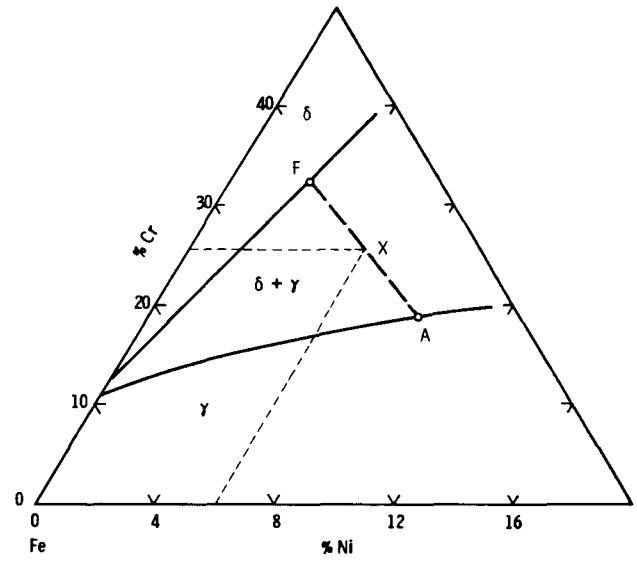

Fig. 10. Isothermal section of Fe-Ni-Cr ternary phase diagram at 1700° F (927° C).

Table IV. Chemical Compositions of Some Duplex Stainless Steels (Wt%; balance: Fe)

Designation	Cr	Ni	Mo	C	N	Cu
Sandvik SAF 2205	22	5.5	3	<0.03	0.12	—
Sumitomo DP 3	25	7	3	—	—	—
Paralloy Sovereign	25	5	3	—	—	2
Ferralium 288	28	8	3	—	0.13	—

Group 5: Face-Centered Cubic, Ferromagnetic Alloys with a Low Curie Temperature

Entirely different categories of materials are based on some of the unique properties of Fe35-pct Ni alloys. These alloys are characterized by both very low coefficients of thermal expansion and low thermoelastic coefficients in the vicinity room temperature. These properties are useful in the manufacture of precision instruments and watches. Other materials used in glass or ceramic seals require a small but controlled thermal expansion from room temperature up to the softening

Table V. Chemical Compositions of the Alloys in Figure 10

Alloy	Cr	Ni	Mn	Si	C	N	Fe
X	25.5	6.0	0.5	0.5	0.08	0.03	Bal.
A	19.5	8.8	0.4	0.4	0.10	0.05	Bal.
F	31.0	3.0	0.6	0.6	0.06	0.02	Bal.

Table VI. Thermal Expansion Coefficients of the Alloys with the Tie-Line Compositions in Figure 10

Pct γ	100	90	80	70	60	53	50	40	0
Pct δ	0	10	20	30	40	47	50	60	100
$\bar{\alpha}$	10.13	9.76	9.40	9.03	8.66	8.40	8.30	7.93	6.46

$\bar{\alpha}$ *RT* to 1000° F (538° C) × 10^{-6}/°F.

point of the glass. Various alloying elements such as Cr, Mo, W, C, Ti, Al, Nb, and Co have been added to Fe-Ni alloys to achieve particular objectives. For example, alloys containing Ti, Al, or Nb can be age-hardened, particularly after cold work, to produce springs with exceptionally high proportional limits.

The anomalously low thermal expansion near room temperature, of the above alloys with approximately 35 pct Ni, has been explained by Seitz [20] and Zener [21] on the basis of magnetic effects taking place near the Curie temperature. The contraction resulting from the loss of the repulsive exchange interaction between atoms, as the Curie temperature is approached on heating, will at least partially counteract the normal thermal expansion arising from increased atomic vibration, thereby giving rise to anomalously low net thermal expansion. Alloying additions can, through their effects on the exchange energy or the Curie temperature, be used to obtain a wide variety of expansion behaviors. Some typical curves of mean thermal expansion coefficient from room temperature to *T* for group 5 alloys are plotted in Figure 5.

Muzyka and Schlosser [22] have developed equations by regression fitting for the median expansion ($\bar{\alpha}$ ~ 3 to 6 × 10^{-6}/°F) ferromagnetic Fe-Ni-Co FCC alloys, which relate $\bar{\alpha}$ and T_c to composition. However, these equations are only applicable for extremely restricted composition ranges. This demonstrates the impracticality of attempting to develop a generalized expression for $\bar{\alpha}$ for all group 5 alloys. The reason the method used for groups 1, 2, and 3 does not work for group 5 alloys is that composition affects both the Curie temperature (magnetic interaction effect) and the basic lattice thermal expansion, and not necessarily in the same way.

Group 5 alloys are generally not adapted to operating at elevated temperatures in severe oxidizing or corrosive environments, because they do not contain Cr or the level of Cr is strictly limited by the strong effect of Cr on the Curie temperature [23,24]. A further restriction to their application is the high Fe content which makes these FCC alloys susceptible to stress-corrosion cracking.

Comparison of the Results of the Modeling Study

To facilitate comparisons between the models for group 1, 2, and 3 alloys, the significant coefficients for the three models are listed in Table II. Fe terms are not applicable (NA) in the Fe-base alloys (groups 1 and 3), and the Ni term is not applicable for group 2 alloys.

Cobalt was present in many group 2 alloys, but its coefficient was both small and not significant. The implication is that Co is comparable to the Ni base as far as $\bar{\alpha}$ is concerned. One might therefore expect the Co coefficient in group 1 stainless steels to be similar to the Ni coefficient, but the level of Co and the number of alloys containing Co in group 1 were too small to provide a significant result. The same situation applies to the W, Ti, Al, and (Nb + Ta) terms in group 1 alloys.

The amounts of Mo, W, (Nb + Ta), and V added to group 3 steels is apparently too small to influence $\bar{\alpha}$ in comparison to the effects of other elements. Mn and N are also not present in significant amounts in these steels.

There is a difference in behavior of Ti, Al, and (Nb + Ta) in group 2 alloys and Ti, Al, and Cu in group 3 steels. In group 2 alloys, these elements are γ′ or γ″ formers, and they decrease $\bar{\alpha}$. In group 3 steels, these additions are made to marginally stable austenites that transform to martensite on cooling or after aging and cooling. The net effect observed is that Ti, Al, and Cu increase $\bar{\alpha}$ in group 3 steels.

To illustrate the application of the regression equations, in Table VII, we have selected 12 common stainless steels, which cover the range of the highest

Table VII. Observed and Predicted TEC 1000 for a Few Commonly Used Group 1 Austenitic Stainless Steels (units of $\bar{\alpha}$: 10^{-6}/°F)

Steel Name	Observed	Predicted	Deviation Obs.-Pred.
Type 202	10.70	10.57	0.13
Nitronic 40	10.60	10.49	0.11
ACI type CF8C	10.30	9.99	0.31
Type 304	10.26	10.22	0.04
Type 316	9.93	10.10	−0.17
A286	9.83	9.68	0.15
ACI type CF8M	9.72	9.90	−0.28
Incoloy 800	9.36	9.39	−0.03
Type 310	9.30	9.64	−0.34
Carpenter 20Nb	9.18	9.42	−0.24
25-20B	9.02	9.21	−0.19
MISCO	8.50	8.79	−0.29

to the lowest TEC 1000, and listed them in the order of decreasing observed $\bar{\alpha}$ from 10.70 to 8.50. The predicted $\bar{\alpha}$ and the deviation are also given. The lowest TEC 1000 in our group 1 steels is 8.50, but this is an arbitrary limit imposed by our definition of group 1 alloys to be restricted to those in which Fe > (Ni + Co). Further lowering of $\bar{\alpha}$ in group 1 alloys by the addition of Mo must be reconciled with increased tendency for sigma phase formation, if the alloy is to be used at elevated temperatures.

Table VIII similarly lists 20 common group 2 Ni-base solid-solution and precipitation-hardening alloys ranging in TEC 1000 from 9.13 to 5.90. The alloys with the lowest $\bar{\alpha}$ are high Ni, high Mo and/or W, and low Cr and Fe. They are not designed for high-temperature service but are rather intended for handling highly corrosive solutions.

The representative group 3 ferritic stainless irons and steels and high-alloy and low-alloy irons and steels listed in Table IX range in TEC 1000 from 8.30 to 6.06. It is apparent that there is a large gap in $\bar{\alpha}$ between the austenitic stainless steels, such as type 304, and a 2-1/4Cr-1Mo or 12 pct Cr ferritic steel. This gap can be filled by selected existing alloys from group 2, or alloys specifically designed for a given application using the model for group 2 alloys as a guide in the selection of alloying elements. Finally, it can be seen in Tables VII, VIII, and IX that the models have been successful in predicting $\bar{\alpha}$ of commercial alloys of interest in all three groups.

Table VIII. Observed and Predicted TEC 1000 for a Few Commonly Used Group 2 FCC Nonmagnetic Ni-Base Alloys (units of $\bar{\alpha}$: 10^{-6}/°F)

Alloy Name	Observed	Predicted	Deviation Obs.-Pred.
N155	9.13	8.73	0.40
S590	8.67	8.48	0.19
Incoloy 901	8.50	8.71	−0.21
D979	8.46	8.20	0.26
Hastelloy X	8.39	8.35	0.04
Refractaloy 26	8.20	8.16	0.04
Inconel 718	8.09	8.27	−0.18
Inconel X-750	8.09	8.14	−0.05
Inconel 600	8.00	8.41	−0.37
Hastelloy R-235	7.90	7.90	0
Inconel 625	7.90	7.80	0.10
Nimonic 80A	7.87	8.10	−0.23
IN 162	7.85	7.59	0.26
Waspaloy	7.85	7.83	0.02
IN 738	7.75	7.68	0.07
Rene 41	7.58	7.46	0.12
M252	7.20	7.55	−0.35
Hastelloy B	6.66	6.60	0
Corronel 220	6.47	6.38	0.09
Chlorimet 2	5.90	6.12	−0.22

Table IX. Observed and Predicted TEC 1000 for a Few Commonly Used Group 3 Ferritic and Martensitic Irons and Steels (units of $\bar{\alpha}$: 10^{-6}/°F)

Steel Name	Observed	Predicted	Deviation Obs.-Pred.
Fortiweld	8.30	7.88	0.42
AISI 1015	8.06	7.90	0.16
0.5Cr-0.5Mo	7.98	7.79	0.19
AISI 4340	7.86	7.69	0.17
$2^1/_4$Cr-1Mo	7.71	7.55	0.16
1Cr-$1^1/_4$Mo-$^1/_4$V	7.74	7.78	−0.02
A213 T22	7.47	7.57	−0.10
Cryonic 5	7.40	7.64	−0.24
$3^1/_2$Ni-$1^3/_4$Cr-$^1/_2$Mo-0.1V	7.25	7.50	−0.25
HY 140	7.18	7.56	−0.38
9Cr-1Mo	7.09	6.84	0.25
17-4 PH	6.77	6.71	0.06
PH 13-8 Mo	6.60	6.38	0.22
HP 9-4-30	6.59	6.73	−0.14
AISI 422	6.55	6.54	0.01
AM 362	6.35	6.48	−0.13
AISI 410	6.34	6.60	−0.26
ALLEG. LUD. 446	6.12	6.38	−0.22
ALLEG. LUD. 29–4	6.06	6.56	−0.50

Limitations of the Modeling Study

The present study of the effects of chemical composition on thermal expansion of various types of alloys was based on published data. As such, it can be no more accurate than the accuracy of the data used in the modeling. Laboratory experience in the experimental measurement of $\bar{\alpha}$ and in the scatter of results reported in the literature for given alloys point out that measurement of $\bar{\alpha}$ requires great attention to experimental technique. Another pitfall in using handbook data and data sheets is that there is usually no indication of whether the results reported for $\bar{\alpha}$ are original measurements or were copied from another source.

Finally, if one were designing an experiment to evaluate the effects of composition on $\bar{\alpha}$, one could take advantage of statistical design to select ranges and combinations of elements so that first- and second-order and interaction terms could be evaluated. In the present instance, we had to accept what data were already available. In the models presented, the absence of a term may only mean that there were insufficient data to establish a significant effect, not that there would be no effect if the element were present in substantial amounts in many of the alloys.

POTENTIAL APPLICATIONS

The possibility of achieving ferritic thermal expansion in high-Cr, high-strength austenitic (FCC) alloys opens up a number of interesting possibilities for design of

alloys to meet various steam turbine material needs for such components as bolts; heavy-walled parts, such as valves, nozzle blocks, and casings; transition joints; valve seat inserts; and composite welded rotors.

Low-Fe and high-Mo alloys of group 2 can have TEC 1000 of less than 8×10^{-6}/°F. The regression equations in Table II provide a guide for the design of alloys with specific thermal expansion characteristics. The principal advantage of such a concept is to provide greatly increased design flexibility in the combined use of austenitic and ferritic alloys in high-temperature structures. Because of the unique and advantageous properties of both ferritic and austenitic alloys, there are many instances in which design benefits would result from combining these materials in the same structure. Unless austenitic and ferritic thermal expansions are matched, problems can arise under three circumstances: maintaining clearances, maintaining interference fits, and minimizing residual or cyclic stresses.

In addition to the aforementioned design advantages, group 2 alloys with TEC 1000 $< 8 \times 10^{-6}$/°F offer two additional benefits. The first is improved resistance to thermal shock compared with austenitic stainless steels, for if other factors are the same, the lower the value of $\bar{\alpha}$, the better is the resistance of the material to thermal shock [26]. Thermal shock is a potential problem in heavy section turbine components as a result of cyclic operation of the turbine and a need for rapid start-up capability. The second benefit is improved resistance to stress-corrosion cracking because of the high Ni and low Fe content.

CONCLUSIONS

From a statistical study on the effect of alloying elements on the thermal expansion coefficient of engineering alloys the following conclusions are made:

1. The mean thermal expansion coefficient from *RT* to 1000° F (538° C) (TEC 1000) was predicted by regression models with a standard error of ± 0.19 to 0.23×10^{-6}/°F for group 1, 2, and 3 alloys.
2. The interstitial elements C and N were found to have a strong per-unit concentration effect on lowering the TEC 1000 of Fe-base nonmagnetic steels; however, the low concentration of C and N results in a small net effect on $\bar{\alpha}$. The most influential elements on $\bar{\alpha}$ for the Fe-base nonmagnetic steels were Ni and Cr, which have a lower per-unit concentration effect but much larger actual concentration present.
3. Mo, W, Ti, Al, (Nb + Ta), and Si decreased, whereas Fe and Mn increased $\bar{\alpha}$ of the Ni-base, FCC, nonmagnetic alloys, the effect of Mo being the strongest. Chromium showed a second-order effect, peaking at 23.6 pct.
4. No particular alloying element other than Cr had a dominating effect on $\bar{\alpha}$ of the ferritic and martensitic irons and steels. The elements that decreased $\bar{\alpha}$ were Cr, Ni, Co, and Si; those that increased $\bar{\alpha}$ were Ti, Al, and Cu.
5. An approximation of $\bar{\alpha}$ of duplex stainless steels can be obtained by using the alloy composition and calculating $\bar{\alpha}$, assuming the structure is all austenitic and using the model for group 1 steels. From this value, one then subtracts 0.037×10^{-6}/°F per percent delta ferrite in the actual microstructure.

ACKNOWLEDGMENTS

The authors acknowledge helpful suggestions made by Dr. J.A. Marshall and Dr. B.J. Shaw on the use of the BMDP statistical computer program and interpretation of the significance of various models. The authors also thank the Electric Power Research Institute for funding the work and for granting us permission to publish the results.

REFERENCES

1. J.M. Wells, S.K. Hwang, and F.C. Hull: Compositional effects on the thermal expansion of iron and nickel base superalloys. J.K. Tien and S.H. Reichman (eds.), *Refractory Alloying Elements in Superalloys*, American Society for Metals, Metals Park, OH, 1984.
2. S.K. Hwang, F.C. Hull, and J.M. Wells: Design of nickel-base superalloys with low thermal expansion coefficient using molybdenum addition, presented at the First USA-Brazil Superalloy Conference, Rio and Araxa, Brazil, April 6–13, 1984.
3. S.K. Hwang, F.C. Hull, and J.M. Wells: Effects of the alloying elements on the thermal expansion coefficient of nonmagnetic Ni-base alloys and austenitic steels, presented at the Fifth International Symposium on Superalloys, Seven Springs, PA, October 1984.
4. S.K. Hwang, F.C. Hull, and J.M. Wells: Thermal expansion of alloys used in power generation, Electric Power Research Institute Final Report, RD-3685, Project 2426-1, Palo Alto, CA, September 1984.
5. *Alloy Digest*, Engineering Alloys Digest, Upper Montclair, NJ.
6. *Metals Handbook*, 9th Ed., vol. 1, pp. 146–147 (1978) and vol. 3, pp. 34–35 (1980), American Society for Metals, Metals Park, OH.
7. *Aerospace Structural Metals Handbook*. Metals and Ceramics Information Center, Battelle's Columbus Laboratories, Columbus, OH.
8. Y.S. Touloukian, R.K. Kirby, R.E. Taylor, and P.D. Desai: *Thermophysical Properties of Matter*, vol. 12; *Thermal Expansion of Elements and Alloys*. IFI/Plenum, New York, 1975.

9. *High Temperature High Strength Nickel Base Alloys.* International Nickel Company, New York, 1964.
10. *Haynes High Temperature Alloys.* Haynes Stellite Company, Kokomo, IN, 1969.
11. W.J. Dixon (ed.): *BMDP Statistical Software.* University of California Press, Berkeley, 1983.
12. H. Morrow III, D.L. Sponseller, and M. Semchyshen: *Met. Trans.*, 1975, vol. 6A, p. 477.
13. H.W. Hayden and S. Floreen: *Trans. Am. Soc. Metals,* 1968, vol. 61, p. 474.
14. S. Floreen and H.W. Hayden: *Trans. Am. Soc. Metals,* 1968, vol. 61, p. 489.
15. H.W. Hayden and S. Floreen: *Met. Trans.*, 1970, vol. 1, p. 1955.
16. L. Kaufman and H. Nesor: *Met. Trans.*, 1974, vol. 5, p. 1618.
17. L. Kaufman and H. Berstein: *Computer Calculation of Phase Diagrams.* Academic Press, New York, 1970.
18. L. Kaufman: *Materials Data Bank Instruction Manual.* Manlabs, Inc., Cambridge, MA, 1976.
19. F.C. Hull: *Symposium Cast Metals for Structural and Pressure Containment Applications,* MPC-11, pp. 205–224. Metals Property Council, New York, 1979.
20. F. Seitz: *The Physics of Metals,* p. 311. McGraw-Hill, New York, 1943.
21. C. Zener: *Trans. AIME,* 1955, vol. 203, p. 619.
22. D.R. Muzyka and D.K. Schlosser: Controlled Expansion Alloy, U.S. Patent 4,006,011, Feb. 1, 1977.
23. L.E. Kindlimann: Austenitic Alloy, U.S. Patent 4,006,012, Feb. 1, 1977.
24. D.F. Smith Jr., E.F. Chatworthy, and D.E. Wenschhof Jr.: Low Expansion Superalloy, U.S. Patent 4,066,447, Jan. 3, 1978.
25. D.F. Smith Jr. and D.E. Wenschhof Jr.: A survey of progress in controlled-expansion, age-hardenable nickel-iron-cobalt alloys. Huntington Alloy Product Division release, Huntington, WV.